Assessment of the manganese cluster's oxidation state via photoactivation of photosystem II microcrystals

Mun Hon Cheah[a,1,2], Miao Zhang[b,1], Dmitry Shevela[c], Fikret Mamedov[a], Athina Zouni[b,2], and Johannes Messinger[a,c,2]

[a]Molecular Biomimetics, Department of Chemistry–Ångström Laboratory, Uppsala University, 75120 Uppsala, Sweden; [b]Institut für Biologie, Humboldt-Universität zu Berlin, 10115 Berlin, Germany; and [c]Department of Chemistry, Chemical Biological Centre, Umeå University, 90187 Umeå, Sweden

Edited by Pierre Joliot, Institut de Biologie Physico-Chimique, Paris, France, and approved November 20, 2019 (received for review September 13, 2019)

Knowledge of the manganese oxidation states of the oxygen-evolving Mn_4CaO_5 cluster in photosystem II (PSII) is crucial toward understanding the mechanism of biological water oxidation. There is a 4 decade long debate on this topic that historically originates from the observation of a multiline electron paramagnetic resonance (EPR) signal with effective total spin of S = 1/2 in the singly oxidized S_2 state of this cluster. This signal implies an overall oxidation state of either $Mn(III)_3Mn(IV)$ or $Mn(III)Mn(IV)_3$ for the S_2 state. These 2 competing assignments are commonly known as "low oxidation (LO)" and "high oxidation (HO)" models of the Mn_4CaO_5 cluster. Recent advanced EPR and Mn K-edge X-ray spectroscopy studies converge upon the HO model. However, doubts about these assignments have been voiced, fueled especially by studies counting the number of flash-driven electron removals required for the assembly of an active Mn_4CaO_5 cluster starting from Mn(II) and Mn-free PSII. This process, known as photoactivation, appeared to support the LO model since the first oxygen is reported to evolve already after 7 flashes. In this study, we improved the quantum yield and sensitivity of the photoactivation experiment by employing PSII microcrystals that retained all protein subunits after complete manganese removal and by oxygen detection via a custom built thin-layer cell connected to a membrane inlet mass spectrometer. We demonstrate that 9 flashes by a nanosecond laser are required for the production of the first oxygen, which proves that the HO model provides the correct description of the Mn_4CaO_5 cluster's oxidation states.

photosynthesis | oxygen evolving cluster | photoassembly | manganese oxidation state | mechanism of water oxidation

Photosynthesis is essential for life as it not only stores solar energy within chemical bonds, but also provides the molecular oxygen required for unlocking the stored energy with high efficiency. The photosynthetic reaction sequence begins with the light-driven oxidation of water that is catalyzed in the biosphere exclusively by PSII. Paradoxically, PSII is also inactivated by light exposure, necessitating a repair process that includes the disassembly and reassembly of the catalytic site for water oxidation in a PSII protein every half hour under full sunlight. Revealing the water oxidation mechanism by PSII, as well as the reassembly process of PSII, is vital for enhancing our knowledge of this key process and may provide inspiration toward the development of artificial water oxidation catalysts needed for the sustainable production of solar fuels, such as hydrogen, ammonia, or methane.

The kinetic scheme describing water oxidation by PSII is known as the Kok cycle (1). It comprises 1 stable (S_1), 3 semistable (S_0, S_2, and S_3), and 1 transient (S_4) intermediate(s) where higher numbers denote successive oxidation of the catalytic center that contains a Mn_4CaO_5 cluster. Recent serial femtosecond X-ray crystallography data provided detailed information about structural changes in the Mn_4CaO_5 cluster as it cycles through the S_0, S_1, S_2, and S_3 states (2, 3), yet the water oxidation mechanism remains controversial (4, 5). One of the long-standing discussion points is the overall oxidation state of the Mn_4CaO_5 cluster (6). Historically, the debate on the Mn oxidation states of the Mn_4CaO_5 cluster arose from the continuous wave X-band electron paramagnetic resonance (EPR) based discovery that the S_2 state gives rise to a multiline signal with an effective total spin of S = 1/2 that has 18–20 hyperfine lines (7, 8). This is a signature of a Mn(III)Mn(IV) mixed valence state within a complex with more than 2 Mn ions, which lead to the overall oxidation state assignments of either $Mn(III)_3Mn(IV)$ or $Mn(III)Mn(IV)_3$ for the Mn_4CaO_5 cluster (6). As recent results confirm that each S-state advancement corresponds to a manganese centered one-electron oxidation (9), the oxidation states for all S-state intermediates in the Kok cycle can be calculated if one of the states is known. Thus, starting from the 2 options for the S_2 state, 2 competing sets of oxidation state assignment have been proposed and are commonly known as the LO or HO models. Subsequent ^{55}Mn electron nuclear double resonance (ENDOR) studies support the assignment of $Mn(III)_3Mn(IV)$ for the S_0 state (10) and of $Mn(III)Mn(IV)_3$ for S_2 (10, 11). The HO model is, furthermore, consistent with recent ^{55}Mn electron–electron double resonance detected NMR (EDNMR) studies of the S_3 state that support the $Mn(IV)_4$ assignment for this state (12). Nonetheless, there are alternative interpretations of the S = 1/2 EPR multiline signal (13) and a ^{55}Mn ENDOR study (14) that supports the LO model.

The oxidation states of the Mn_4CaO_5 cluster have been studied over the past 3 decades by a large number of additional techniques. Mn K-edge X-ray absorption near edge structure (15–17) and Mn Kβ X-ray emission spectroscopy (XES) (9, 15, 18) studies

Significance

Photosynthetic water oxidation by the multisubunit membrane protein complex PSII is an important process that sustains all aerobic life on Earth by producing molecular oxygen from sunlight and water. Understanding the mechanism of this process is crucial toward advancing fundamental knowledge as well as providing a blueprint for the development of solar fuel devices. Important pieces of information required for solving the mechanism of biological water oxidation are the oxidation states of the manganese ions forming the catalytic site of water oxidation in PSII. Here, we resolve a long-standing controversy between 2 competing schools of thought, by providing a clear-cut determination of overall manganese oxidation states using a simple counting experiment.

Author contributions: M.H.C., M.Z., D.S., A.Z., and J.M. designed research; M.H.C., M.Z., D.S., and F.M. performed research; M.H.C. and F.M. analyzed data; and M.H.C., M.Z., D.S., F.M., A.Z., and J.M. wrote the paper.

The authors declare no competing interest.

This article is a PNAS Direct Submission.

Data deposition: All data discussed in the paper are available at http://uu.diva-portal.org under accession no. diva2:1368663.

[1]M.H.C. and M.Z. contributed equally to this work.

[2]To whom correspondence may be addressed. Email: michael.cheah@kemi.uu.se, athina.zouni@hu-berlin.de, or johannes.messinger@kemi.uu.se.

This article contains supporting information online at https://www.pnas.org/lookup/suppl/doi:10.1073/pnas.1915879117/-/DCSupplemental.

First published December 17, 2019.

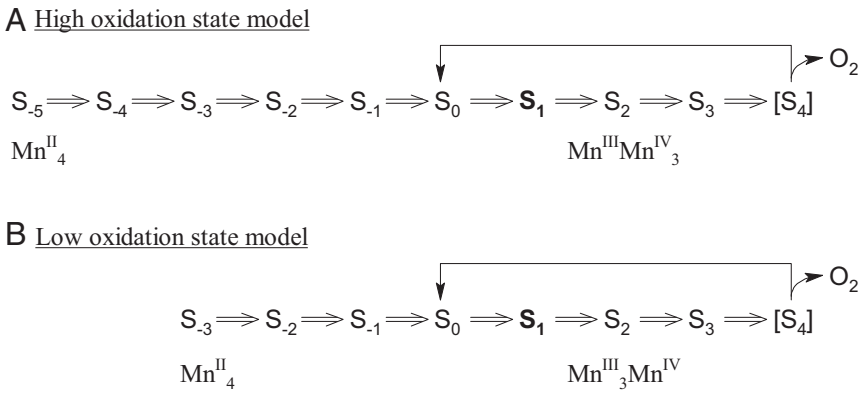

Fig. 1. Schematic of photoactivation of PSII based on the (*A*) high oxidation model and (*B*) low oxidation model. S_0–S_4 states are intermediate states of the Kok cycle; S_{-5} to S_{-1} states are photoactivation intermediate states. The dark stable S_1 state is labeled in bold. Each double arrow corresponds to a flash-induced one-electron oxidation.

by various groups unanimously support the HO model. Yet these studies are challenged by alternative interpretations (19, 20) that suggest that the available data are better suited toward the LO model.

Beyond spectroscopic methods, the oxidation state of Mn_4CaO_5 can be inferred by an inventory of the redox equivalence between the Mn^{2+} and the functional Mn_4CaO_5 cluster. Titration of reductant to functional Mn_4CaO_5 while monitoring the amount of Mn^{2+} formation (21) or the progressive shift of the first maximum in flash-induced oxygen oscillation patterns allow assessments of the overall oxidation states (22, 23). Most of these data have been interpreted to support the HO model, but the study by Kretschmann et al. (23) supports the LO model.

The converse approach is the photooxidation of exogenously supplied Mn^{2+} by PSII depleted of the Mn_4CaO_5 cluster (apo-PSII) to restore O_2-evolving functionality in a process known as photoactivation (refs. 24–33; for reviews, see refs. 34 and 35). When using single turnover flashes, the photooxidation of Mn is a one-electron oxidation event as seen, for example, in intact dark-adapted (S_1 state) PSII samples where such an illumination leads to a period 4 oscillation with the first O_2 evolution after the third flash (1, 36, 37). Thus, by counting the number of single turnover flashes required to evolve the first O_2 during photoactivation of apo-PSII, the overall oxidation state of the Mn_4CaO_5 cluster can be established. Starting from exogenously supplied Mn^{2+}, O_2 evolution after 7 flashes corresponds to the LO model, while O_2 evolution after 9 flashes corresponds to the HO model (see Fig. 1). In contrast to the majority of the results presented above, previous reports of the oxidation state determination via photoactivation support the LO model (33, 35, 38). However, the light flashes used in these studies were not strictly single turnover but rather consisted of trains of short LED pulses. While these flashes, which were employed for increasing the yield of photoactivation to a level that O_2 evolution could be detected, were designed by taking independently determined kinetics of the photoactivation process into account (33), this opens the possibility of multiple oxidation's per flash. One indication for this may be the unexpected observation of O_2 evolution below the minimum number of 7 light flashes (33).

Recently, a crystal structure of a Mn-depleted PSII core complex from *Thermosynechococcus elongatus* was reported at 2.55 Å resolution that is based on a complete depletion of the Mn_4CaO_5 cluster in PSII crystals via NH_2OH and EDTA treatments (39). Importantly, the resulting apo-PSII crystals retained all 20 protein subunits, including the 3 extrinsic proteins that stabilize the Mn_4CaO_5 cluster. This preparation of highly purified and well-defined apo-PSII crystals present a new opportunity to assess the overall oxidation state of Mn_4CaO_5 by photoactivation. In this paper, we use this preparation in combination with saturating nanosecond (ns) laser pulses that fully exclude multiple oxidation's of the reaction center's during one flash. Highly sensitive detection of the evolved O_2 was achieved by a thin-layer membrane inlet cell (Fig. 2) that was connected to an isotope ratio mass spectrometer (IRMS). This unique experimental design enabled us to detect O_2 release after the first $S_3 \rightarrow [S_4] \rightarrow S_0$ transition reached during photoactivation. Consequently, the oxidation state determination did not require any complicated analysis beyond the straightforward count of the number of laser flashes required to observe O_2 evolution.

Results and Discussion

Flash-induced oxygen release patterns (FIOPs) of PSII microcrystals of *T. elongatus* core preparations were recorded at 20 °C in the presence of the artificial electron acceptor phenyl-*p*-benzoquinone (PPBQ) employing a thin-layer membrane inlet mass spectrometry (MIMS) cuvette (Fig. 2) and nanoseconds duration green (532 nm) laser flashes. The FIOPs of native PSII microcrystals (blue trace in Fig. 3) exhibited the typical period 4 oscillation of dark-adapted PSII samples with maxima at the third, seventh, and 11th flashes. The damping of this oscillation can be described by a miss parameter of 10%, which demonstrates that the laser light was saturating and that the exogenous electron acceptor allowed sustaining oxygen evolution well beyond the number of flashes needed to determine the overall Mn oxidation state of the oxygen-evolving complex. The excellent oscillation is remarkable given the fact that, due to the slow mass transport of O_2 from the MIMS cuvette into the ion source of the IRMS, the laser flashes were spaced 15 s apart to resolve individual flash-induced oxygen peaks. In this context, we note that the small oxygen yield after the second flash is not due to double oxidation of a minor

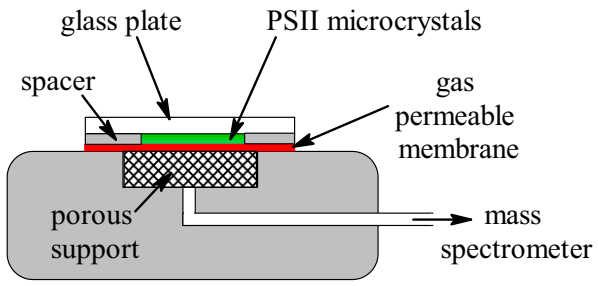

Fig. 2. Schematic of the thin-layer membrane inlet mass spectrometer cuvette. The sample is confined within a 6-mm-diameter chamber that has a height of 100 μm.

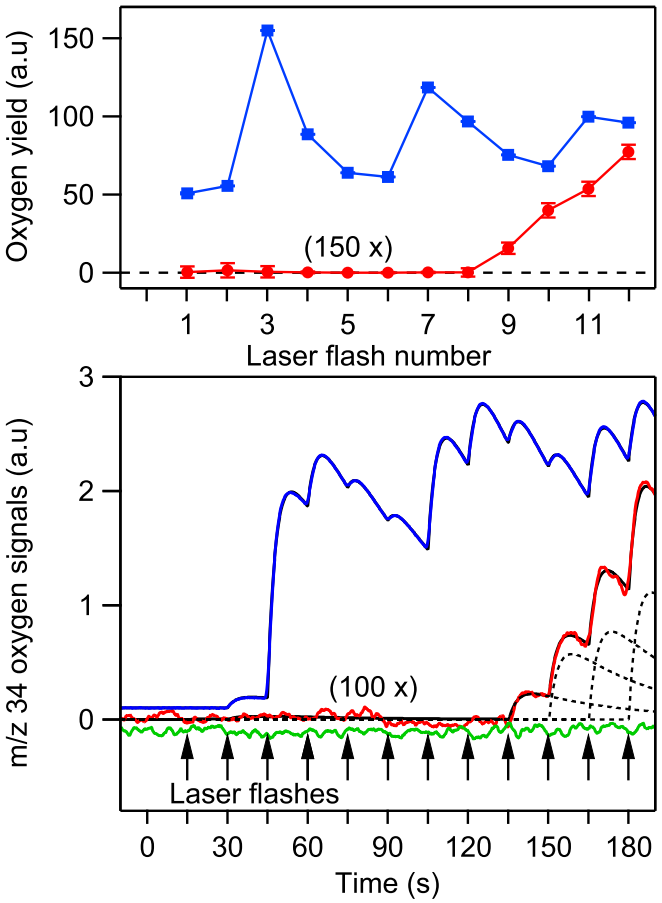

Fig. 3. (*Top*) Representative FIOPs of native PSII microcrystals (blue trace) and during the photoactivation of apo-PSII microcrystals using equal flash spacings of 15 s (red trace). The red trace magnified by 150 times; the blue trace offset from zero for clarity. Error bars are 95% confidence interval derived from the fitting procedure and smaller than the marker symbols. (*Bottom*) Original oxygen signals from the MIMS system during laser flashing of apo-PSII microcrystals incubated in an assembly buffer (red trace); apo-PSII microcrystals without Mn^{2+} and Ca^{2+} (green trace) and a native PSII microcrystal (blue trace). The dashed line: fitted oxygen peaks after each laser flash; the black line: sum of all fitted oxygen peaks. The vertical arrows indicate laser flashes. The red and green traces are magnified by 100 times. The green and blue traces were offset from zero for clarity.

fraction of PSII centers (double hits) but to the extremely long S_2 and S_3 state lifetimes in the presence of PPBQ that led to an incomplete S_1 state synchronization within the 60 min dark-adaptation period after the preflash employed to oxidize tyrosine D (40–44).

The green trace obtained with Mn-free (Fig. 3) apo-PSII microcrystals in the absence of added Mn^{2+} and Ca^{2+} but with the exogenous electron acceptor PPBQ shows that, in contrast to initial trials with Clark and Joliot type electrodes, the laser pulses did not cause any flash-induced artifacts in the MIMS system. Importantly, no O_2 was produced by apo-PSII in the absence of added Mn and Ca cofactors.

On the basis of these controls, photoactivation experiments were performed by adding 10 mM $MnCl_2$, 400 mM $CaCl_2$, 5 mM $NaHCO_3$, and the same acceptor as above (assembly buffer) to dark-adapted apo-PSII microcrystals (no preflash treatment), which were then flashed in the same way as above. No molecular oxygen was observed in the first 8 flashes, but the ninth flash induced a clearly resolved O_2 signal indicating the successful assembly of the Mn_4CaO_5 cluster in a fraction of the centers (red trace in Fig. 3). The subsequent rise of the flash-induced O_2 signal shows the photoactivation of further PSII centers. It does not display any oscillation, indicating a significant miss factor causing mixing of S states during photoactivation.

The O_2 yield after the ninth flash was ~0.1% of that obtained from native PSII microcrystals after the third flash, indicating that the S_1 state population was 0.1% after 6 photoactivation flashes. This implies that the average quantum yield of photoactivation for the first 6 flashes is close to 32% (*SI Appendix*), i.e., higher than the typically reported quantum yield of 1% based on noncrystalline Mn_4CaO_5 depleted PSII preparations (24, 25, 27, 28, 34). This comparison also allows the estimation that the absolute O_2 yield induced by the ninth flash was about 15 nM, i.e., well above the estimated oxygen detection limit of 3 nM in the current experimental setup (*SI Appendix*, Figs. S1 and S2). We note that the observation of O_2 evolution after 9 flashes can be made consistent with the LO model if the O_2 patterns of photoactivation are shifted by 2 electrons due to the presence of auxiliary electron donors that donate electrons more efficiently to Y_Z^{ox} or $P680^+$ than Mn. The most likely auxiliary electron donors are tyrosine D, Y_D, and cytochrome *b* 559, cyt b_{559}. However, this scenario is considered highly unlikely due to the presence of a high affinity Mn^{2+} binding site at or near the assembled Mn_4CaO_5 cluster involving the D1-A170 and D1-E333 residues (29, 45–47). Transient variable fluorescence (48, 49) and EPR measurements (49, 50) during single flash experiments on Mn depleted PSII samples have demonstrated that electron donation from this specifically bound Mn^{2+} to Y_Z^{ox} is very efficient. This is expected given the much longer distances (>30 Å) of Y_D or cyt b_{559} as compared to Mn^{2+} at the high affinity binding site (7 Å). Moreover, the rate of Y_Z oxidation by $P680^+$ at pH < 7 is, at least, 2 orders of magnitude faster compared to the oxidation of Y_D or cyt b_{559} based on optical and EPR measurements in Mn depleted PSII samples (51, 52).

According to the two-quantum model of photoactivation (25, 34), a second photon is required to stabilize the intermediate formed after the first flash; the optimal flash spacing between the first and the second flash is reported to be between 0.5 and 1 s. Thus, the long dark time (15 s) between flashes used above may allow significant back reaction of the first photooxidized intermediate, potentially reducing the O_2 yield that may originate from the seventh flash to below our detection limit. In the results presented in Fig. 4, we, therefore, applied a modified flash sequence in which a preflash train was used with 0.5 s spacing (green), followed by a dark time of 240 s before a second flash train (15 s spacing, red) was applied. This modified flash sequence should allow optimal formation of the 2-photon stabilized intermediate by minimizing the amount of back reaction thereby allowing the detection of O_2 evolution from the seventh flash (if any). For apo-PSII microcrystal suspensions that were subjected to 2 preflashes (2PF), the total number of flashes (sum of preflashes and flashes) required to evolve O_2 was, however, still 9, further supporting the HO model (Fig. 4). This test additionally excludes the scenario where residual NH_2OH that remained in the samples after 10 washing steps, calculated to be below 0.1 μM (*SI Appendix*), leads to back reactions of photoactivation intermediates between the dark times of the flashes. We further confirmed this observation by examining the sum of flashes required to evolve O_2 from apo-PSII that were subjected to 0PF to 8PF. Between 0PF and 6PF, in total, 9 laser flashes were required in each case to evolved O_2 and the O_2 yields induced by the ninth flash were similar in each case (blue symbols in Fig. 4). At 6PF, 7PF, and 8PF, the number of additional laser flashes (red) required to evolve O_2 remained constant at 3 flashes, while the O_2 yield increased with each additional preflash. These observations can be rationalized by the formation of the S_1 state after 6PF and of the S_2 and S_3 states after 7PF and 8PF, which decay back to the dark stable S_1 during the 240 s dark

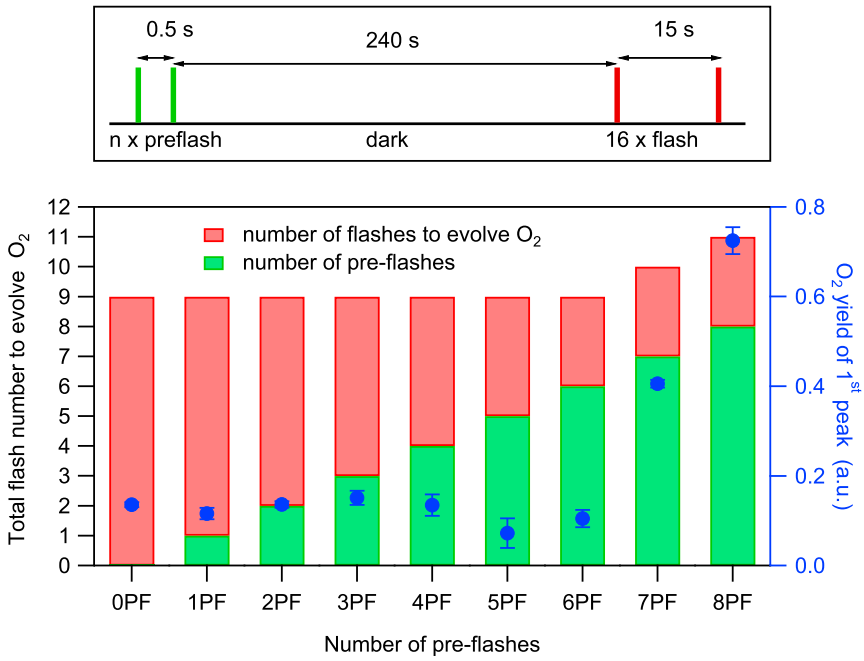

Fig. 4. (*Top*) Laser flash spacing's used for photoactivation of apo-PSII microcrystals suspension by various combinations of tightly spaced preflashes (green line) and monitoring flashes (red line) with 15-s spacing. The dark time of 240 s was employed to allow the back reaction of the S_2 and S_3 states to S_1. (*Bottom*) Total number of flashes required to observe the first O_2 evolution (left axis) during the photoactivation of apo-PSII crystals with various combinations of preflashes and monitoring flashes (see *Top*). The yields of the first O_2 peaks, plotted in blue, are the averages of 2 repeat measurements, and the error bars are SDs.

time via electron donation by, for example, tyrosine Y_D (see below). Therefore, 3 additional flashes were required in each case to complete the first catalytic cycle to evolve O_2, and the larger number of total flashes led to the expected increased photoactivation yields (compare to Fig. 3). EPR experiments showed that, in the dark-adapted apo-PSII samples, indeed, 94% of Y_D was reduced due to the NH_2OH treatment (*SI Appendix*, Fig. S4). Thus, the data in Fig. 3 provide additional strong evidence that the S_2 state was formed for the first time after 7 flashes and that the first O_2 was produced after 9 flashes during the first $S_3 \rightarrow [S_4] \rightarrow S_0$ transition.

To summarize, in contrast to previous photoactivation studies that employed complicated LED pulse trains as flashes, our data obtained with single turnover ns-laser pulses provides strong support for the HO state model of the Mn_4CaO_5 cluster. Together with the spectroscopic evidence for the HO model, this provides the required firm basis for deriving the mechanism of water oxidation. Furthermore, this study demonstrates the feasibility of the stepwise photoactivation of the Mn_4CaO_5 cluster depleted PSII microcrystals, which will allow detailed time resolved structural characterization of photoactivation intermediates using serial femtosecond X-ray crystallography.

Materials and Methods

T. elongatus cells were cultivated, and PSII core complexes purified as described previously (39). Intact PSII microcrystals with a size between 20 and 80 μm were generated according to literature methods (53). Apo-PSII microcrystals were obtained as in ref. 39 by incubating intact PSII microcrystals for 30 min with 50 mM NH_2OH and 50 mM EDTA, but the crystals were, subsequently, washed 8 times and dialyzed 2 times to achieve rigorous removal of NH_2OH and EDTA. The estimated residual NH_2OH and EDTA concentrations are no more than 0.1 μM (*SI Appendix*). EPR spectra of the apo-PSII microcrystal suspension in the $g = 2.0$ region were completely devoid of features associated with Mn^{2+} before and after heat treatment at 363 K to release any residual Mn, confirming the complete absence of Mn in apo-PSII preparations (*SI Appendix*, Fig. S3).

The apo-PSII microcrystals were stored in 0.1 M MES pH 6.5, 0.1 M NH_4Cl, and 20% PEG 5000 (MIMS buffer). All manipulations of apo-PSII microcrystals were performed in complete darkness with the aid of an IR camera and 940 nm illumination. Apo-PSII microcrystal suspensions (0.5 ± 0.15 mM) in an assembly buffer (MIMS buffer with 10 mM $MnCl_2$, 400 mM $CaCl_2$, 5 mM $NaHCO_3$, and 0.3 mM PPBQ, 6% $H_2{}^{18}O$) were confined within a 6 mm diameter chamber that is 100 μm thick (thin-layer MIMS cuvette; Fig. 2) and allowed to degas for 4 min. Saturating single turnover flashes were provided using a 10 ns duration laser (532 nm and 60 mJ/cm^2 per pulse). The thin-layer MIMS cuvette was connected to the source vacuum of a Thermo Delta XP IRMS via a dry ice/ethanol cooling trap (54). Oxygen evolution was monitored via the *m/z* 34 signal from the IRMS. The oxygen yield for each flash-induced peak was calculated using a multipeak fitting procedure implemented in the software Igor Pro-6.3 (WaveMetrics) (for details see the *SI Appendix*).

Data Availability Statement. All data discussed in the paper are available at http://uu.diva-portal.org under accession number diva2:1368663.

ACKNOWLEDGMENTS. We thank Casper de Lichtenberg and Gesine Bartels for technical assistance. This project was supported by the Swedish Research Council (Grant 2016-05183). A.Z. and M.Z. acknowledge financial support funded by the Deutsche Forschungsgemeinschaft (DFG, German Research Foundation) under Germany's Excellence Strategy- EXC 2008/1 - 390540038.

1. B. Kok, B. Forbush, M. McGloin, Cooperation of charges in photosynthetic O_2 evolution-I. A linear four step mechanism. *Photochem. Photobiol.* **11**, 457–475 (1970).
2. M. Suga *et al.*, Light-induced structural changes and the site of O=O bond formation in PSII caught by XFEL. *Nature* **543**, 131–135 (2017).
3. J. Kern *et al.*, Structures of the intermediates of Kok's photosynthetic water oxidation clock. *Nature* **563**, 421–425 (2018).
4. D. A. Pantazis, Missing pieces in the puzzle of biological water oxidation. *ACS Catal.* **8**, 9477–9507 (2018).
5. W. Lubitz, M. Chrysina, N. Cox, Water oxidation in photosystem II. *Photosynth. Res.* **142**, 105–125 (2019).
6. V. Krewald *et al.*, Metal oxidation states in biological water splitting. *Chem. Sci.* **6**, 1676–1695 (2015).
7. G. C. Dismukes, Y. Siderer, Intermediates of a polynuclear manganese center involved in photosynthetic oxidation of water. *Proc. Natl. Acad. Sci. U.S.A.* **78**, 274–278 (1981).
8. Ö. Hansson, L.-E. Andréasson, EPR-detectable magnetically interacting manganese ions in the photosynthetic oxygen-evolving system after continuous illumination. *Biochim. Biophys. Acta Bioenerg.* **679**, 261–268 (1982).
9. I. Zaharieva *et al.*, Room-temperature energy-sampling K_β X-ray emission spectroscopy of the Mn_4Ca complex of photosynthesis reveals three manganese-centered oxidation steps and suggests a coordination change prior to O_2 formation. *Biochemistry* **55**, 4197–4211 (2016).

10. L. V. Kulik, B. Epel, W. Lubitz, J. Messinger, Electronic structure of the Mn_4O_xCa cluster in the S_0 and S_2 states of the oxygen-evolving complex of photosystem II based on pulse ^{55}Mn-ENDOR and EPR spectroscopy. *J. Am. Chem. Soc.* **129**, 13421–13435 (2007).
11. J. M. Peloquin *et al*., ^{55}Mn ENDOR of the S_2-state multiline EPR signal of photosystem II: Implications on the structure of the tetranuclear Mn cluster. *J. Am. Chem. Soc.* **122**, 10926–10942 (2000).
12. N. Cox *et al*., Photosynthesis. Electronic structure of the oxygen-evolving complex in photosystem II prior to O-O bond formation. *Science* **345**, 804–808 (2014).
13. M. Zheng, G. C. Dismukes, Orbital configuration of the valence electrons, ligand field symmetry, and manganese oxidation states of the photosynthetic water oxidizing complex: Analysis of the $S(_2)$ state multiline EPR signals. *Inorg. Chem.* **35**, 3307–3319 (1996).
14. L. Jin *et al*., Electronic structure of the oxygen evolving complex in photosystem II, as revealed by ^{55}Mn Davies ENDOR studies at 2.5 K. *Phys. Chem. Chem. Phys.* **16**, 7799–7812 (2014).
15. J. Messinger *et al*., Absence of Mn-centered oxidation in the S(2) –> S(3) transition: Implications for the mechanism of photosynthetic water oxidation. *J. Am. Chem. Soc.* **123**, 7804–7820 (2001).
16. H. Dau, P. Liebisch, M. Haumann, X-ray absorption spectroscopy to analyze nuclear geometry and electronic structure of biological metal centers–Potential and questions examined with special focus on the tetra-nuclear manganese complex of oxygenic photosynthesis. *Anal. Bioanal. Chem.* **376**, 562–583 (2003).
17. M. Haumann *et al*., Structural and oxidation state changes of the photosystem II manganese complex in four transitions of the water oxidation cycle (S0 –> S1, S1 –> S2, S2 –> S3, and S3,4 –> S0) characterized by X-ray absorption spectroscopy at 20 K and room temperature. *Biochemistry* **44**, 1894–1908 (2005).
18. K. M. Davis *et al*., X-ray emission spectroscopy of Mn coordination complexes toward interpreting the electronic structure of the oxygen-evolving complex of photosystem II. *J. Phys. Chem. C* **120**, 3326–3333 (2016).
19. R. J. Pace, L. Jin, R. Stranger, What spectroscopy reveals concerning the Mn oxidation levels in the oxygen evolving complex of photosystem II: X-ray to near infra-red. *Dalton Trans.* **41**, 11145–11160 (2012).
20. S. Petrie, R. Stranger, R. J. Pace, What Mn K_β spectroscopy reveals concerning the oxidation states of the Mn cluster in photosystem II. *Phys. Chem. Chem. Phys.* **19**, 27682–27693 (2017).
21. T. Kuntzleman, C. F. Yocum, Reduction-induced inhibition and Mn(II) release from the photosystem II oxygen-evolving complex by hydroquinone or NH_2OH are consistent with a Mn(III)/Mn(III)/Mn(IV)/Mn(IV) oxidation state for the dark-adapted enzyme. *Biochemistry* **44**, 2129–2142 (2005).
22. J. Messinger, G. Seaton, T. Wydrzynski, U. Wacker, G. Renger, $S_{(-3)}$ state of the water oxidase in photosystem II. *Biochemistry* **36**, 6862–6873 (1997).
23. H. Kretschmann, H. T. Witt, Chemical reduction of the water splitting enzyme system of photosynthesis and its light-induced reoxidation characterized by optical and mass spectrometric measurements: A basis for the estimation of the states of the redox active manganese and of water in the quaternary oxygen-evolving S-state cycle. *Biochim. Biophys. Acta Bioenerg.* **1144**, 331–345 (1993).
24. G. M. Cheniae, I. F. Martin, Photoactivation of the manganese catalyst of O 2 evolution. I. Biochemical and kinetic aspects. *Biochim. Biophys. Acta* **253**, 167–181 (1971).
25. R. Radmer, G. M. Cheniae, Photoactivation of the manganese catalyst of O_2 evolution. II. A two-quantum mechanism. *Biochim. Biophys. Acta Bioenerg.* **253**, 182–186 (1971).
26. G. M. Cheniae, I. F. Martin, Effects of hydroxylamine on photosystem II: II. Photoreversal of the NH(2)OH destruction of O(2) evolution. *Plant Physiol.* **50**, 87–94 (1972).
27. N. Tamura, G. Cheniae, Photoactivation of the water-oxidizing complex in photosystem II membranes depleted of Mn and extrinsic proteins. I. Biochemical and kinetic characterization. *Biochim. Biophys. Acta Bioenerg.* **890**, 179–194 (1987).
28. M. Miyao-Tokutomi, Y. Inoue, Improvement by benzoquinones of the quantum yield of photoactivation of photosynthetic oxygen evolution: Direct evidence for the two-quantum mechanism. *Biochemistry* **31**, 526–532 (1992).
29. G. M. Ananyev, G. C. Dismukes, High-resolution kinetic studies of the reassembly of the tetra-manganese cluster of photosynthetic water oxidation: Proton equilibrium, cations, and electrostatics. *Biochemistry* **35**, 14608–14617 (1996).
30. G. M. Ananyev, G. C. Dismukes, Assembly of the tetra-Mn site of photosynthetic water oxidation by photoactivation: Mn stoichiometry and detection of a new intermediate. *Biochemistry* **35**, 4102–4109 (1996).
31. S. V. Baranov *et al*., Bicarbonate is a native cofactor for assembly of the manganese cluster of the photosynthetic water oxidizing complex. Kinetics of reconstitution of O_2 evolution by photoactivation. *Biochemistry* **43**, 2070–2079 (2004).
32. H. J. Hwang, R. L. Burnap, Multiflash experiments reveal a new kinetic phase of photosystem II manganese cluster assembly in Synechocystis sp. PCC6803 in vivo. *Biochemistry* **44**, 9766–9774 (2005).
33. D. R. J. Kolling, N. Cox, G. M. Ananyev, R. J. Pace, G. C. Dismukes, What are the oxidation states of manganese required to catalyze photosynthetic water oxidation? *Biophys. J.* **103**, 313–322 (2012).
34. H. Bao, R. L. Burnap, Photoactivation: The light-driven assembly of the water oxidation complex of photosystem II. *Front. Plant Sci.* **7**, 578 (2016).
35. J. Dasgupta, G. M. Ananyev, G. C. Dismukes, Photoassembly of the water-oxidizing complex in photosystem II. *Coord. Chem. Rev.* **252**, 347–360 (2008).
36. P. Joliot, G. Barbieri, R. Chabaud, Un nouveau modeles des centres photochimiques du systeme II. *Photochem. Photobiol.* **10**, 309–329 (1969).
37. P. Joliot, B. Kok, "Oxygen evolution in photosynthesis" in *Energetics of Photosynthesis*, Govindjee, Ed. (Elsevier, 1975), pp. 387–412.
38. L. Zaltsman, G. M. Ananyev, E. Bruntrager, G. C. Dismukes, Quantitative kinetic model for photoassembly of the photosynthetic water oxidase from its inorganic constituents: Requirements for manganese and calcium in the kinetically resolved steps. *Biochemistry* **36**, 8914–8922 (1997).
39. M. Zhang *et al*., Structural insights into the light-driven auto-assembly process of the water-oxidizing Mn_4CaO_5-cluster in photosystem II. *eLife* **6**, e26933 (2017).
40. B. A. Diner, Dependence of the deactivation reactions of Photosystem II on the redox state of plastoquinone pool a varied under anaerobic conditions. Equilibria on the acceptor side of Photosystem II. *Biochim. Biophys. Acta Bioenerg.* **460**, 247–258 (1977).
41. J. H. A. Nugent, C. Demetriou, C. J. Lockett, Electron donation in photosystem II. *Biochim. Biophys. Acta Bioenerg.* **894**, 534–542 (1987).
42. W. F. J. Vermass, A. W. Rutherford, O. Hansson, Site-directed mutagenesis in photosystem II of the cyanobacterium *Synechocystis* sp. PCC 6803: Donor D is a tyrosine residue in the D2 protein. *Proc. Natl. Acad. Sci. U.S.A.* **85**, 8477–8481 (1988).
43. L. V. Pham, J. Messinger, Probing S-state advancements and recombination pathways in photosystem II with a global fit program for flash-induced oxygen evolution pattern. *Biochim. Biophys. Acta* **1857**, 848–859 (2016).
44. S. Styring, A. W. Rutherford, Deactivation kinetics and temperature dependence of the S-state transitions in the oxygen-evolving system of Photosystem II measured by EPR spectroscopy. *Biochim. Biophys. Acta Bioenerg.* **933**, 378–387 (1988).
45. M. Asada, H. Mino, Location of the high-affinity $Mn(^{2+})$ site in photosystem II detected by PELDOR. *J. Phys. Chem. B* **119**, 10139–10144 (2015).
46. P. J. Nixon, B. A. Diner, Aspartate 170 of the photosystem II reaction center polypeptide D1 is involved in the assembly of the oxygen-evolving manganese cluster. *Biochemistry* **31**, 942–948 (1992).
47. K. A. Campbell *et al*., Dual-mode EPR detects the initial intermediate in photoassembly of the photosystem II Mn cluster: The influence of amino acid residue 170 of the D1 polypeptide on Mn coordination. *J. Am. Chem. Soc.* **122**, 3754–3761 (2000).
48. M. L. Ghirardi, T. W. Lutton, M. Seibert, Interactions between diphenylcarbazide, zinc, cobalt, and manganese on the oxidizing side of photosystem II. *Biochemistry* **35**, 1820–1828 (1996).
49. T. A. Ono, H. Mino, Unique binding site for Mn^{2+} ion responsible for reducing an oxidized YZ tyrosine in manganese-depleted photosystem II membranes. *Biochemistry* **38**, 8778–8785 (1999).
50. C. W. Hoganson, D. F. Ghanotakis, G. T. Babcock, C. F. Yocum, $Mn(^{2+})$ reduces Y_z^+ in manganese-depleted photosystem II preparations. *Photosynth. Res.* **22**, 285–293 (1989).
51. C. A. Buser, L. K. Thompson, B. A. Diner, G. W. Brudvig, Electron-transfer reactions in manganese-depleted photosystem II. *Biochemistry* **29**, 8977–8985 (1990).
52. P. Faller *et al*., Rapid formation of the stable tyrosyl radical in photosystem II. *Proc. Natl. Acad. Sci. U.S.A.* **98**, 14368–14373 (2001).
53. M. Ibrahim *et al*., Improvements in serial femtosecond crystallography of photosystem II by optimizing crystal uniformity using microseeding procedures. *Struct. Dyn.* **2**, 041705 (2015).
54. K. Beckmann, J. Messinger, M. R. Badger, T. Wydrzynski, W. Hillier, On-line mass spectrometry: Membrane inlet sampling. *Photosynth. Res.* **102**, 511–522 (2009).